



Assessing solar heating of binders to be applied in roofs, roads or heat collectors

R. Álvarez-Barajas, B. García-Márquez, C. Delgado-Sánchez, A.A. Cuadri, F.J. Navarro and P. Partal

Pro2TecS-Chemical Process and Product Technology Research Centre, Department of Chemical Engineering, ETSI.
Campus de “El Carmen”, Universidad de Huelva, 21071, Huelva, (Spain)

Abstract.

Enhancing the energy efficiency of buildings, roads, or other applications involves, as a main challenge, the development of innovative materials with customised thermomechanical properties and thermal energy capabilities while maintaining cost-effectiveness. These materials can be designed to find application as solar heat absorbers or to prevent issues related to urban heat island. To that end, a reliable assessment of the material behaviour under solar irradiation is required. With this aim, this work proposed an experimental setup that has been simulated by CFD and built to test different bituminous and non-bituminous binders with potential use in roofing, road and heat collectors.

Key words. Bitumen, non-bituminous binder, solar behaviour, CFD.

1. Introduction

The scarcity of fossil fuels and the high energy consumption of non-renewable energy sources have become significant concerns for the sustainability of energy and climate change. The high consumption of fossil fuels has directly led to carbon dioxide emissions, which have severely impacted energy crises and global warming. According to Eurostat, the residential sector accounts for 27.2% of final energy consumption in the European Union. The majority of this energy consumption is attributable to natural gas (36.0%) and electricity (24.1%), with renewables accounting for a mere 17.5%. The analysis further reveals that the heating of space and water accounts for an astounding 78.9% of the final energy consumed by households, with space heating accounting for more than 64.0% of this total [1].

Bitumen, a by-product of crude oil distillation, is a highly viscous liquid or solid at room temperature, black or dark brown in colour, and characterised by a very complex molecular composition. The properties of bitumen, including its low cost, impermeability, strength, and elasticity, make it a suitable material for use in civil engineering applications such as paving or waterproofing membranes for building applications [2]. In addition, and

related to its black colour, its low albedo and high solar absorptivity makes bitumen a promising material that would play the role of the black absorber plate in the flat plate solar collector.

Conversely, such solar characteristics make materials made of bitumen responsible for the well-known urban heat island effect. In this regard, light colour/pigmentable non-bituminous binders have arisen as a promising alternative to reduce such issues. Their ability to reflect solar radiation may be used to both reduce the urban heat island effect and to enhance their thermal performance and overall energy efficiency [3, 4]. Therefore, enhancing the energy efficiency poses a significant challenge, the development of innovative materials with customised thermomechanical properties and thermal energy capabilities while maintaining cost-effectiveness.

These materials can be designed depending on their final application as solar heat absorbers or to prevent issues related to urban heat island. To that end, a reliable assessment of material behaviour under solar irradiation is required. With this aim, this work proposed an experimental setup that has been CFD simulated and built to test different bituminous and non-bituminous binders with potential in roofing, road and heat collectors.

2. Methodology

Bituminous binders (neat and SBS-modified bitumens) were tested, ranging softening point between 50 and 120°C and penetrations between 20 and 70 dmm. Non-bituminous binders were formulated with the following base components: a rosin ester; a waste vegetable cooking oil; and a polymer (e.g. EVA, LDPE, HDPE/PP, crumb rubber from discarded tyres, etc.) to obtain the desired in-service performance, depending on the target application.

Solar irradiation setup was built to simulated solar irradiation using a Xenon lamp HXF300-T3 (Beijing China Education Au-light Technology Co., Ltd, China) with an attached filter AM 1.5G (300-1100 nm). Testing

specimens consisted of a binder disk (42 mm diameter and 8.5 mm thickness) with 5 temperature sensors located at different positions, four of them at the centre ($r=0$ mm) with readings at different depths and one close to the sample wall (Fig. 1). An additional temperature reading was recorded in close proximity to the sample wall ($r=20.925$ mm and $x=2.36$ mm). The sample side wall was isolated with an insulator measuring 77.6 mm in thickness ($k=0.044$ W/m °C, thermal conductivity), whereas its bottom side was in contact with an isothermal heat sink, with selected cooling or sink temperatures (T_s).

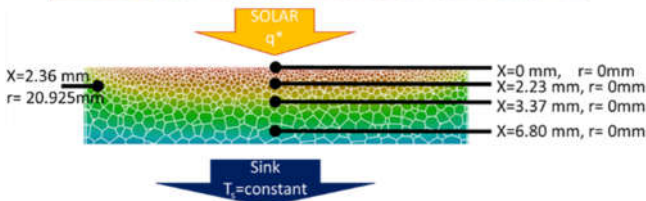
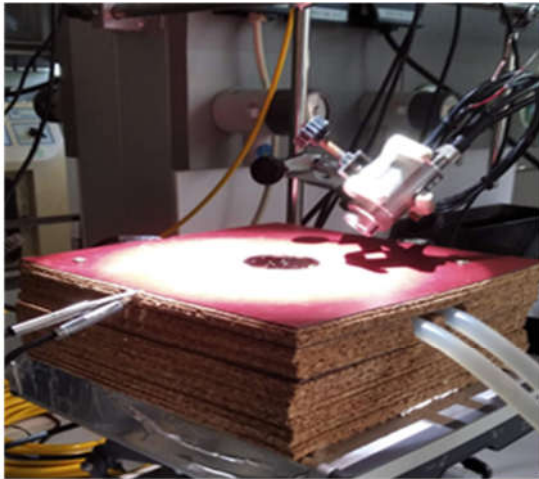


Fig. 1. General view of the experimental setup for solar irradiation simulations. Location of temperature sensors inside the sample.

Thermal conductivity tests using the Transient Hot-Bridge (THB) technique and a Type A metal-framed sensor (A-13890) were carried out between 20 and 60°C in a THB 100 instrument from Linseis GmbH (Germany).

3. Results and discussion

Experiential solar irradiation setup was simulated by Computational Fluid Dynamics (CFD) using Fluent-Ansys CFD 2020 software. A mesh containing approximately 470000 polyhedral cells was used for this analysis (Fig. 2).

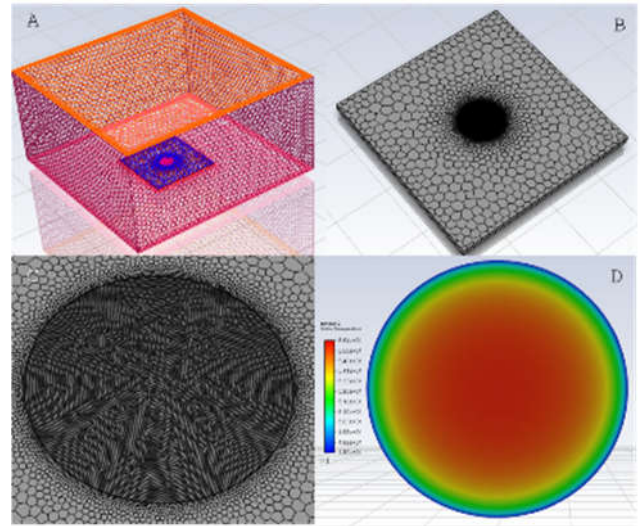


Fig. 2. CFD simulation of the experimental: Meshing (A, B, C) and temperature distribution on sample top surface (D).

For a selected bitumen and solar heat flux on sample top surface, CFD simulation estimates that around 10% energy is reflected by the sample, in agreement with the bitumen albedo, 0.1. The other 90% effective solar heat flux is partially conducted through the top surface of the bituminous sample ($\approx 35\%$) and lost between binder and the environment due to thermal radiation ($\approx 20\%$) and natural convection ($\approx 35\%$) (Fig. 3). Additionally, simulations estimate that about 29% of heat conducted towards the sink is lost through the insulator.

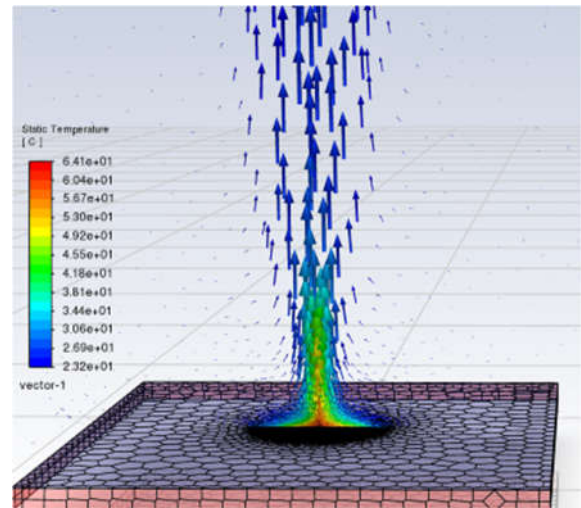


Fig. 3. Heat loss due to free convection.

Simulations were compared with the experimental patterns of recorded temperatures upon irradiation (Fig. 4 and 5). They show a rapid increase of the top surface temperature, followed by the other temperatures, towards equilibrium temperatures that decrease as the distance from the top increases. CFD simulation predicts fairly well experimental steady state temperatures recorded along the sample centre and at the specimen wall (Fig. 5).

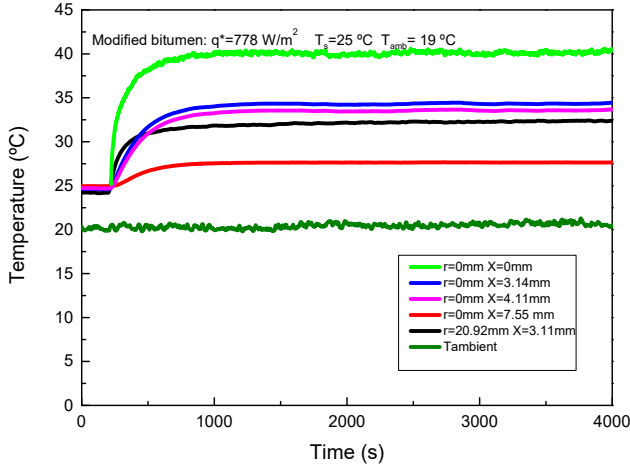


Fig. 4. Temperatures recorded at different sample positions with irradiation time.

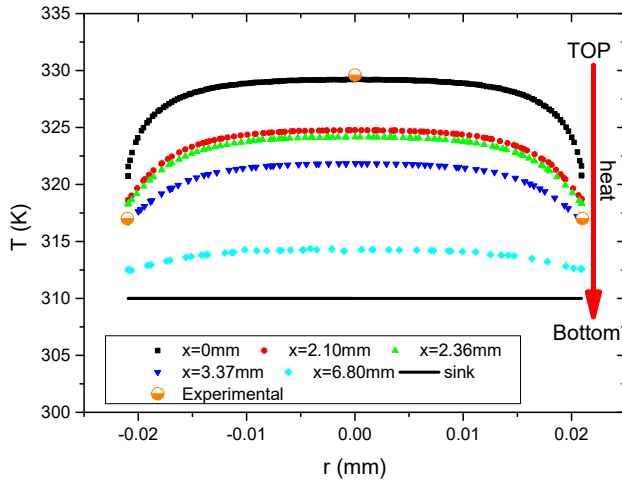


Fig. 5. CFD-simulated temperature profiles a function of sample radius (r) and depth (x).

These steady state temperatures will be used to obtain local heat flux conducted through sample, by means of the Fourier's law:

$$q'_{cond}(r=0mm) = -k \frac{dT}{dx} \quad (1)$$

where k is the material thermal conductivity and x is related to the position of the recorded temperatures.

As illustrated in Fig. 6, the thermal conductivity (k) values of the materials under investigation are shown as a function of temperature. As can be observed, the thermal conductivities of the materials exhibit minimal variation within the designated experimental temperature range. Notably, modified bitumen demonstrates an average value of $0.13 \text{ W/m}^\circ\text{C}$, which is lower than those values obtained for the dark and light colour non-bituminous binders, which have an average value of $k=0.19 \text{ W/m}^\circ\text{C}$ and $k=0.15 \text{ W/m}^\circ\text{C}$, respectively.

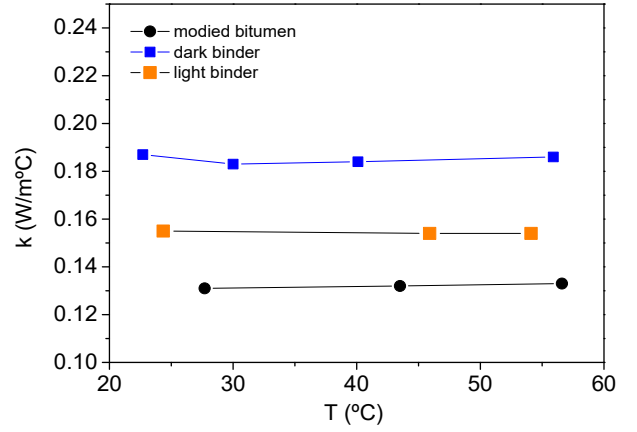


Fig. 6. Material thermal conductivities.

Finally, material solar heat absorption capability, q_{abs} , was calculated, as follows:

$$q_{abs}(\%) = \frac{q'_{cond}(r=0mm)}{q^*_{r=0mm}} \times 100 \quad (2)$$

by comparing conducted local heat flux (Eq. 1) with the irradiated local heat flux ($q^*_{r=0mm}$). Table 1 gathers results obtained for selected binders.

As may be seen in Table 1, binders can be customised to exhibit the desired solar behaviour, contingent on the intended application. In general, bitumen-based materials have been found to demonstrate a higher capacity for heat absorption, which makes them promising candidates for use in novel heat solar collectors.

Table 1. Local heat flux conducted through the sample and material solar heat absorption as a function of local irradiated heat flux.

Sample	Test conditions	$q'_{cond}(r=0mm)$ (W/m ²)	q_{abs} (%)
Modified Bitumen	$q^*=778 \text{ W/m}^2$ $T_s = 25 \text{ }^\circ\text{C}$ $T_{amb}=19 \text{ }^\circ\text{C}$	248	32
Modified bitumen	$q^*=1050 \text{ W/m}^2$ $T_s = 35 \text{ }^\circ\text{C}$ $T_{amb}=19.5 \text{ }^\circ\text{C}$	294	28
Binder dark	$q^*=778 \text{ W/m}^2$ $T_s = 19 \text{ }^\circ\text{C}$ $T_{amb}=19 \text{ }^\circ\text{C}$	227	29
Light colour	$q^*=1050 \text{ W/m}^2$ $T_s = 35 \text{ }^\circ\text{C}$ $T_{amb}=19.5 \text{ }^\circ\text{C}$	205	19.5

Conversely, non-bituminous binders can be designed with light colour to reduce the heat solar absorption (e.g. up to around 20%) of roofs or roads (i.e. to mitigate the urban heat island effect) or with dark/black colour to replace bitumen in applications requiring high absorptivity, with a similar solar heat absorption to bituminous products, around 30% absorption.

However, heat absorption capability of a material will depend on the selected test (or environmental) conditions (Table 2).

Table 2. Local heat flux conducted through the dark non-bituminous binder and its material solar heat absorption as a function environmental conditions: Irradiation heat (q^*), sink temperature (T_s), ambient temperature (T_{amb}) and sample top temperature (T_{top}).

Solar Irradiation	T_s (°C)	T_{amb} (°C)	T_{top} (°C)	q_c (W/m ²)	q_{abs} (%)
Modified bitumen					
$q^*=1030$ W/m ²	32	23.27	53.5	354	33.2
$q^*=1030$ W/m ²	36.7	21.3	56.68	332	31.2
$q^*=1030$ W/m ²	42.8	22.6	56.1	239	22.4
Dark binder					
$q^*=1030$ W/m ²	37.5	21.5	52.3	327.6	31.8
$q^*=760$ W/m ²	37.5	23.5	49.1	256.6	33.8
$q^*=570$ W/m ²	37.5	24.4	44.7	167.0	29.8
$q^*=450$ W/m ²	37.5	24.2	42.2	117.0	26.3
$q^*=570$ W/m ²	20	20.3	33.6	276.0	48.4
$q^*=570$ W/m ²	10	22.2	24.3	270.2	47.4

As gathered in Table 7, the conduction of heat through the sample increase with the Sun's altitude or angle throughout the day, corresponding to the lowest intensity, $q^*=450$ W/m², at an angle of 30° and the highest intensity, $q^*=1030$ W/m², at an angle of 80° [5]. Likewise, under a selected experimental conditions for the dark binder ($T_s=37.5^\circ\text{C}$), the heat absorbed (or conducted) by the non-bituminous binder (q_{abs}) tends to decrease as applied irradiation does. Conversely, if irradiation intensity is kept constant at 1032 W/m² for the modified bitumen or 570 W/m² for the dark binder, Table 2 shows that q_{abs} decreases as the sink temperature (T_s) is raised.

As commented above, irradiation tests and calculated heat absorbed by the material result from the following energy balance:

$$q^*_{r=0mm} \times \text{Albedo} = q'_{cond} + q'_{CN} + q'_{Rad} \quad (3)$$

where q'_{cond} , q'_{CN} and q'_{Rad} are, respectively, the conducted, free convection and radiation heat fluxes. Equation 3 can be rewritten as,

$$\frac{q^*_{r=0mm} \times \text{Albedo}}{q'_{cond}} = 1 + \frac{q'_{CN}}{q'_{cond}} + \frac{q'_{Rad}}{q'_{cond}} \quad (4)$$

that can be simplified to

$$\frac{1}{q_{abs}(\%)} \approx \frac{q'_{CN}}{q'_{cond}} + \text{constant} \quad (5)$$

or

$$\frac{1}{q_{abs}(\%)} \approx \frac{h}{k/\Delta x} \cdot \frac{T_{top}-T_{amb}}{T_{top}-T_s} + \text{constant} \quad (5)$$

where h is the convection heat transfer coefficient, k the thermal conductivity and Δx the sample thickness.

Fig. 7 shows calculated values of Equation 5. As may be seen the final heat absorption strongly depends on selected experimental conditions (i.e. on the environmental condition at which material is subjected), and mainly, on the ratio between free convection and conducted heat fluxes.

Thus, for a given material, heat absorption is higher if ambient and sample top temperatures are closed or by decreasing sink temperature.

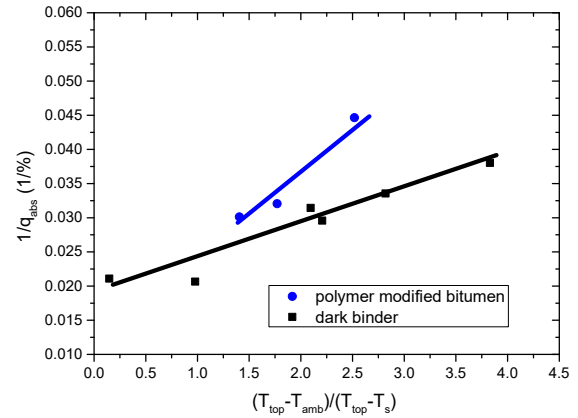


Fig. 7. Dependence of the heat absorbed by the sample on the ratio between free convection and conducted heat fluxes.

Finally, it is noteworthy that these experimental results, calculated with local heat fluxes (i.e. temperatures recorded at $r=0\text{mm}$), are in good agreement with the average values predicted by CFD, despite the aforementioned non-uniform temperature distribution within the sample and calculated heat losses through the insulator.

4. Conclusion

Obtained results showed that binders can tailored with desired solar behaviour, according to the target application. As a whole, bitumen-based materials exhibit a higher heat absorption capability, being promising products for use in novel heat solar collectors. On the other hand, non-bituminous binders may be designed with light colour to reduce the heat solar absorption of roofs or roads (i.e. to mitigate urban heat island effect) or with dark/black colour to replace bitumen in applications requiring high absorptivity.

Acknowledgement

This work is part of the project PID2023-149701OA-I00 funded by MCIN/AEI/10.13039/501100011033 (Spanish Ministry of Science, Innovation and Universities) and ERDF "A way of making Europe". C. Delgado-Sánchez acknowledges financial support from the EMERGIA research program (DGP_EMEC_2023_00091) from Consejería de Universidad, Investigación e Innovación (Junta de Andalucía).

References

- [1] A. Serrano Durán M, Dauvergne JL, Doppiu S, Del Barrio EP, Sol Energy Mater Sol Cells 220 (2021) 110848.
- [2] D. Lesueur (2009), Adv. Colloid Interface Sci 145 42-82.
- [3] R. Álvarez-Barajas, Cuadri, A.A., Delgado-Sánchez, C., Navarro, F. J., Partal, P. (2023). Journal of Cleaner Production, 393, 136350.
- [4] R. Álvarez-Barajas, Cuadri, A.A., Delgado-Sánchez, C., Navarro, F. J., Partal, P. (2024). Polymer Testing, 130, 108317.
- [5] J.P. Holman (1997). Heat Transfer, eight edition, McGraw-Hill Inc, New York,